NASA TECHNICAL MEMORANDUM 102694

THE INFLUENCE OF MICROSTRUCTURE ON THE TENSILE BEHAVIOR OF AN ALUMINUM METAL MATRIX COMPOSITE

Michael J. Birt and W. Steven Johnson

JULY 1990

National Aeronautics and Space Administration

Langley Research Center
Hampton, Virginia 23665-5225

Summary

The relationship between tensile properties and microstructure of a powder metallurgy aluminum alloy, 2009 has been examined. The alloy was investigated both unreinforced and reinforced with 15 v/o or 30 v/o SiC whiskers or 15 v/o SiC particulate to form a discontinuous metal matrix composite (MMC). The materials were investigated in the as-fabricated condition and in three different hot-rolled sheet thicknesses of 6.35, 3.18 and 1.8mm. Image analysis was used to characterize the morphology of the reinforcements and their distributions within the matrix alloy. Fractographic examinations revealed that failure was associated with the presence of microstructural inhomogeneities which were related to both the matrix alloy and to the reinforcement. The results from these observations together with the matrix tensile data were used to predict the strengths and moduli of the MMC's using relatively simple models. The whisker MMC could be modeled as a short fiber composite and an attempt was made to model the particulate MMC as a dispersion/dislocation hardened alloy.

Introduction

Discontinuous silicon-carbide (SiC) aluminum metal matrix composites (MMC's) are under consideration as candidate materials for aerospace/aeronautical applications. They have a potential for weight saving over conventional aluminum alloys as they exhibit improved specific strength and stiffness values over those of the matrix alloy and can be fabricated by conventional means. However, the effects of discontinuous SiC additions on the strengthening of aluminum alloys are not well understood, although a number of mechanics/microstructural models have been proposed to account for the observed property improvements.

Arsenault and his co-workers [1,2] have shown that a high dislocation density exists in discontinuous SiC-aluminum MMC's as a result of the thermal stresses generated upon quenching from the solution heat treatment temperatures. These stresses arise due to the large difference between the coefficients of thermal expansion of the reinforcement and the matrix. The dislocations produced promote a higher degree of strain hardening through dislocation interactions during deformation which may increase the ultimate strength of the MMC's. However, it is difficult to quantify the number and effectiveness of these dislocations on composite strengthening.

In an early review of the then available data, Nair et al [3] observed that the moduli and strengths of several discontinuous aluminum MMC's could be predicted using a simple rule-of-mixtures approach if the length/diameter ratios of the fibers were known. Lederich and Sastry [4] combined the flow stress for a SiC-aluminum MMC (determined by the rule-of-mixtures) with the calculated stress required for Orowan looping of the particles by dislocations and found that these superimposed stresses could more clearly describe the strengthening contribution of the SiC particles than calculations based on the rule-of-mixtures alone. Nardone and Prewo [5], have suggested that a shear-lag model modified to incorporate load transfer to the fiber ends by the matrix can more accurately correlate discontinuous SiC-aluminum tensile data than models based on dislocation strengthening or particle strengthening theories. The shear lag model which they propose requires the presence of a strong fiber/matrix interface, a phenomenon which has been observed in 2XXX series SiC reinforced aluminum MMC's

[6,7]. Therefore, at the present time there exist several models which have been successfully used to describe microstructural/tensile property relationships for these materials.

This paper compares the effects of discontinuous SiC particulate (SiCp) and whisker (SiCw) additions on the tensile properties of an Al-Cu-Mg alloy in the as-fabricated condition. It is shown that both the strengths and the moduli of the MMC's can be accurately predicted using simple models based on microstructural considerations.

Experimental Techniques

Materials

The materials were obtained both with and without reinforcement from the Advanced Composite Materials Corp.(ACMC). The unreinforced matrix alloy was 2009 which had a nominal composition of 4.0% Cu, 1.4% Mg, 0.02% Fe, Balance Al and was produced as a powder by a gas atomization process. The MMC's contained either 15 volume percent (v/o) particulate or 15 or 30 v/o whiskers. The particulate was produced from single crystals of abrasive grade α-SiC that had been crushed into powder and sieved. The whiskers were a complex mixture of α-β SiC grown from rice hulls and designated F-9 by ACMC. Nominally the whiskers contain a mixture of 80 v/o whiskers and 20 v/o whisker debris [8].

All four of the materials were vacuum hot-pressed above the solidus temperature (490°C) into 152 mm diameter billets, extruded to rectangular 127 x 12.7 mm sheets and hot-rolled to the required sheet thickness. The whisker MMC's were rolled perpendicular to the extrusion direction to a sheet thickness of 6.35mm. Next they were rolled parallel to the extrusion direction to 3.18 mm and then perpendicular to the extrusion direction to 1.8mm. The particulate MMC and the unreinforced matrix alloy were rolled perpendicular to the extrusion direction to 6.35mm and then successively rolled parallel to the extrusion direction in the 3.18 and 1.8mm sheets. All other manufacturing processes are proprietory. Representative microstructures of the 15 v/o particulate and whisker MMC's in the 1.8mm sheet thickness are shown in Figures 1 and 2, respectively.

Mechanical Testing

Due to the limited supply of materials tensile data were restricted to the results of either duplicate or single tests from each sheet of material in the L-T and T-L orientations. Where 'L'

is the extrusion direction and 'T' is normal to 'L'. Care was taken to use specimens taken from the center of the plates where this was practical. Tests were conducted in laboratory air at room temperature at a constant strain rate of 5×10^{-4} sec^{-1} and the test specimen geometry is shown in Figure 3.

Microstructural Characterization

The microstructures of the materials in all three sheet thicknesses were examined in a scanning electron microscope (SEM) using both secondary and back-scattered electron imaging. Specimens for these investigations were prepared by mechanically polishing small sections of each sheet followed by etching using Kellers reagent.

Image analysis was used to characterize the lengths and diameters of the particulates and whiskers. To determine the effects of hot-rolling on the whisker MMC's, the distribution of whisker orientations relative to the extrusion direction (L) was determined by image analysis using 15° orientation increments between 0°, the extrusion direction, and 90°. There was no measurable out-of-plane whisker orientation distribution relative to the through-thickness direction. Due to their irregular morphology a comparison of the size distributions of the particulate was made by determining cross-sectional areas of individual particles lying on the three orthogonal faces of each sheet.

Fractography

Failure mechanisms were determined by SEM examinations of fractured halves of tensile specimens. An energy dispersive X-ray (EDX) analysis system was used to determine the elemental composition of second phase particles present in the materials. Image analysis was used to characterize the fracture surface topography.

Results and Discussion

Microstructure

The microstructures of the MMC's were inhomogenous and consisted of fine grains of the matrix alloy interspersed with non-uniform bands of the SiC reinforcement as shown by the example in Figure 4. This type of banded microstructure has been observed in a 20 v/o SiCw 6061 Al alloy [9] and has been shown to adversly affect the ductility of these materials [10]. In

the present study hot-rolling reduced the banding, however, there was no noticeable improvement in the ductilities of the MMC's, due to inconsistences in the data.

The whisker MMC's contained microstructural irregularities which were not present in the particulate MMC's; these included unbonded whiskers and voids associated with whisker clusters associated with poor mixing and non-infiltration by the matrix alloy during hot-pressing. An example of this is shown in Figure 5. Such features have been reported in earlier generation materials by Nieh et al [9] and Crowe et al [11] and more recently by Harris and Wawner [6]. The hot-rolling process partially sealed the non-infiltrated regions in the whisker MMC's and as a result of breaking up the reinforcements, produced a distribution of particulate sizes, whisker lengths and whisker orientations with respect to the extrusion axis for each reduction in sheet thickness. These distributions are presented in Figures 6 and 7 and Table I.

Figures 6 and 7 show the image analysis data obtained for the whisker orientation distributions and average whisker lengths of the 15 v/o and 30 v/o SiCw MMC's, respectively. The whiskers tend to become preferentially aligned with respect to the extrusion direction during the extrusion process and the results indicate that >25% of the whiskers in the 15 v/o SiCw sheets and >20% in the 30 v/o SiCw sheets retain their alignment after hot-rolling. There is a marginal decrease in the average whisker length with decreasing sheet thickness in both of the MMC's as a result of whisker breakage. Also, the whiskers are more readily broken-up in the 30 v/o MMC due to their closer packing and the increased likelihood of contact between the brittle whiskers resulting in whisker breakage. Average sizes of the SiC particulates in the 15 v/o SiCp MMC are shown in Table I. These results illustrate that the particulate reinforcement is similarly broken up by hot-rolling.

Tensile Properties

Tensile data for the four materials are presented in Table II. Since the measured strain hardening exponents were significantly greater for the MMC's than for the matrix alloy, a 0.2% offset yield stress would not be truly representative of the yield stress. Measured strain hardening exponents in the 6.35mm sheet thickness in the L-T orientation increased from the matrix value of 0.11 to 0.15, 0.23 and 0.48 for the particulate, 15 v/o whisker and 30 v/o whisker MMC's, respectively.

The preferential alignment of the materials following extrusion might be expected to cause some anisotropy of the tensile properties of the whisker MMC's and this is apparent in the 15 v/o SiCw MMC. However, the rolling procedures have largely eliminated the effects of preferred orientation in the other materials.

The addition of the SiC reinforcements has influenced the tensile properties of the MMC's over those of the matrix. In most instances the particulates and whiskers improve the ultimate strengths of the base Al alloy as a result of the high volume fraction of reinforcement (15-30 v/o) which promotes dislocation/reinforcement interactions. This is illustrated by the higher work hardening rates of the MMC's over those of the matrix alloy. The proportional limit is not substantially affected by the reinforcement additions.

There is no direct correlation between reinforcement volume fraction and strength. The high density of dislocations and the large volume fraction of SiC in the MMC's would be expected to strongly influence the strengths of the MMC's by providing a greater number of heterogenous nucleation sites available for precipitates. The aging response of aluminum alloys has been shown to be accelerated by the addition of discontinuous SiC reinforcements; by promoting earlier precipitate nucleation in the MMC's than in the unreinforced matrix alloy [12,13]. However, the effect of this accelerated aging on the strength of the MMC's has yet to be determined. In the present study the 30 v/o SiCw MMC exhibits strength values which are in several instances lower than those of the 15 v/o SiCw or SiCp. The reasons for this are complex and are possibly due the presence of microstructural inhomogeneities, differences in the whisker lengths resulting from whisker breakage and to the effects of whisker clustering and voids which make whisker/matrix separation easier. The ultimate strength and proportional limit of the particulate MMC are much higher than expected in the 3.18mm sheet and the reason for this anomalous behavior is unclear, but it is probably associated with the fabrication process.

The ductilities of the MMC's are considerably reduced primarily as a result of the high volume fraction of the SiC reinforcement which prevents stress relaxation and promotes high local stresses within the matrix material [8]. The plastic strain distribution within the matrix of the 30 v/o MMC will be different to that of the 15 v/o SiCw MMC due to the greater degree of

constraint in the higher volume fraction MMC which will tend to lower the plastic strain in this material [14]. Conversely, the constraint in the particulate MMC will be lower than that in the whisker MMC's due to the much smaller size and more spherical geometry of the particulate compared to the whiskers which would raise the plastic strain. From this argument it might be expected that elongations to failure would be much lower in the 30 v/o whisker MMC and highest in the particulate MMC, however, the data is inconclusive.

The addition of SiC whiskers and particulates increases the moduli of the MMC's but the effect is non-linear and the whisker MMC's have been shown to obey an isostress relationship as reported by McDanels [8]. The 30 v/o SiC whisker MMC shows approximately a 100% increase in modulus in the longitudinal direction over the unreinforced matrix. Whisker breakage due to fabrication reduces this value as the sheet thickness decreases from 6.35 to 1.8mm. The whiskers appear to be marginally more effective at increasing the elastic modulus than the particulates at the same volume fraction in the L-T orientation. The observed increase in the L-T moduli of the whisker MMC's over the particulate MMC is expected as the much larger aspect ratio of the whiskers (> 18) over the particulate (~ 1-2) will permit more effective load transfer to the whiskers. Similarly, the transverse moduli of the 15 v/o particulate and whisker MMC's are comparable because the hexagonal whisker cross-section approximates the shape of a particulate whose aspect ratio is approximately unity.

Fractography

Fracture in the materials was often associated with microstructural inhomogeneities. SEM fractography frequently revealed the presence of large particles of the matrix alloy on the fractured surfaces of the tensile specimens in both the unreinforced matrix alloy and in the MMC's, as shown by the example in Figure 8. These large particles are probably a result of the gas atomization process which may produce large droplets of the Al alloy and concomitantly large powder particles. This observation together with the presence of numerous copper-rich areas determined by EDX analysis within the matrix of the materials, would tend to suggest that either the batch of master alloy powder was of poor quality or that the blending was poor.

Several failure mechanisms associated with Al-MMC's have been identified in the literature. They are largely dependent upon the matrix alloy and aging condition, reinforcement

morphology and volume fraction. The commonly observed failure modes are particle cracking, fracture within the matrix and particle/matrix interface debonding [15,16,17].

The fractured surfaces of the MMC's are shown in Figures 8 to 11. First appearances tend to suggest that fracture has occured by void coalescence, which occurs in the unreinforced matrix alloy. However, upon closer examination the dimples in the MMC's are shallow and in many cases are flattened. The reason for the shallow appearance of the dimples is due to the high volume fraction of the reinforcement which produces constraint within the matrix material as shown by Christman et al [14]. The reason for the flattened dimples may be a result of separation along well dispersed prior particle boundaries of the order of 2-5μm. A pre-existing oxide film commonly occurs on the surface of atomised aluminum-based powders and has been reported to exist in SiC/Al MMC's by Nutt [18]. This oxide film embrittles the prior particle boundaries causing premature failure and the flattened dimpled morphology. The 30 v/o SiCw MMC exhibited numerous areas of brittle, cleavage fracture on the surfaces. It has been shown that discontinuous reinforcement additions of 30-40 v/o SiC produce a more brittle appearance to the fracture surfaces of Al-MMC's [8]. The particulate MMC exhibited a similar fracture surface morphology to that of the whisker MMC's consisting of shallow dimples. Few SiC particles were observed on the fracture surfaces, however, larger SiC particulate particles, >4μm were occasionally observed where these had debonded as shown in Figure 9. The absence of SiC particles on the fracture surfaces suggests that failure occured within the matrix between the reinforcing particles and implies that particle/matrix bonding is good.

In several instances the tips of whiskers were observed to protrude a short distance (<2μm) from the base of dimples in the whisker MMC's, as shown in Figure 10, which would imply that a void had formed at the whisker end. There was evidence of a thin layer of matrix material attached to these whiskers, as illustrated in Figure 11, which would suggest that the fracture path was through the matrix adjacent to the whiskers. Arsenault and Pande [19] have observed the occurence of protruding whiskers coated with matrix material on the fracture surfaces of a SiCw reinforced 6061 aluminum alloy. They showed that the aluminum diffuses into the whiskers from the matrix and as a result this strengthens the whisker/matrix interface.

Modeling and Predictions

A number of authors have attempted to correlate the strengths of discontinuously reinforced SiC/Al-MMC's using the traditional particle strengthening theories which are applied where strengthening is due to the presence of sub-micron precipitates and fine dispersions in unreinforced Al alloys. It is questionable if such theories can be applied to particles of the order of 1 - 100μm in size. However, it could similarly be argued that particles have too low an aspect ratio to be considered a true fiber reinforcement. It can be shown that if the ratio of the average whisker length/critical whisker length (l_i/l_{crit}) equals 10 for a discontinuously reinforced composite then 95% of the strength of a continuously reinforced composite will be achieved [20]. The SiCw MMC's in the present study contained whiskers whose average lengths yielded (l_i/l_{crit}) ratios which were 2-3; hence, these whiskers could not be considered as effective a reinforcement as a continuous fiber. The tensile strength of a discontinuously reinforced MMC possessing a distribution of whisker lengths can be estimated from the following equation if it is assumed that the whiskers are uniformly dispersed in the matrix and aligned in the direction of loading [21]:

$$\sigma_{uc} = \sum^{l_1 \geq l_{crit}} \sigma_{uf} V_{f_1} \left(1 - \frac{l_{crit}}{2\, l_1} \right) + \sum^{l_2 < l_{crit}} V_{f_2} \tau_m \frac{l_2}{d} + \sigma'_{um} \left(1 - V_f \right) \qquad (1a)$$

where:

$$l_{crit} = \frac{\sigma_{uf}\, d}{2\, \tau_m} \qquad (1b)$$

σ_{uc} = ultimate composite strength

σ_{uf} = ultimate whisker strength

V_{f_1} = volume fraction of whiskers > l_{crit}

l_{crit} = critical whisker length

l_1 = average length of whiskers ≥ l_{crit}

l_2 = average length of whiskers < l_{crit}

d = average whisker diameter

V_{f_2} = volume fraction of whiskers < l_{crit}

τ_m = shear strength of the matrix

V_f = total whisker volume fraction

σ'_{um} = unreinforced matrix strength at the failure strain of the MMC

If the case of the 15 v/o (actual value 15.8 v/o) SiCw, 6.35mm thick sheet is considered then σ_{uf} = 3.45GPa [22], V_{f1} = 0.1205, l_{crit} = 5.8μm, l_1 = 16.09μm, l_2 = 5.62μm, d = 0.52μm, V_{f2} = 0.0059, τ_m = 154MPa, V_f = 0.126 (assuming that the reinforcement is 80 v/o whiskers and the remainder is debris), and σ'_{um} = 236MPa. Using these values, equation (1a) yields a value of 557MPa for the ultimate strength of the MMC. There is, however, a distribution of off-axis whiskers in the 15 v/o SiCw MMC with orientations between 0-90° with respect to the loading direction as shown in Figure 6. Only ~25% of the whiskers are oriented within 15° of the loading direction resulting in a lower experimental value of 432MPa. A more accurate estimate of the strength of the MMC can be obtained using the data from Figure 6 and assuming that each orientation increment of 15° between 0-90° contains the same distribution of whisker lengths. The strength contributions from whiskers within each orientation increment can then be approximated from the strength of an individual whisker, σ_x of average length l_1 or l_2 transformed with respect to its orientation to the loading direction. The stress in the whisker transformed in this manner, σ_x' can be calculated from the relationship:

$$\sigma_x' = \sigma_x \cos^2\theta \qquad (2a)$$

where: σ_x = the ultimate strength of the whisker (3.45GPa)

θ = the orientation of the whisker with respect to the extrusion direction

and:
$$\sigma_{uf} = \sum_{\theta=0°}^{\theta=90°} \sigma_x' \qquad (2b)$$

The strength contributions of the whiskers within each 15° increment can be found from equation (2b) and substituted in equation (1a) to give the composite strength. This approach using the mean angle of whisker orientation for each 15° increment, which reduces σ_{uf}, gives a value of 429MPa and is close to the experimental data. The predictions shown in Figure 12 for the L-T orientations are largely conservative and, although the model is simple, the

correlation is good. The exception is the 30 v/o SiCw MMC in the 6.35mm sheet thickness, this is possibly due to the numerous whisker clusters, voids and other microstructural irregularities in this material discussed earlier.

Neglecting the 1st term in equation (1a) and substituting data for the particulate MMC, the predicted strengths fall ~ 19-44% below the actual data. The modified shear lag theory proposed by Nardone and Prewo [5] similarly underestimates the strengths of the SiCp MMC by as much as 35%. The strength of the particulate MMC is difficult to reconcile with the shear lag theories above as the particles are of too low an aspect ratio and approach the case of a high volume fraction dispersion hardened alloy more closely than a whisker or a short fiber MMC.

Arsenault [23] has shown that the strengths of the SiCw / 6061 Al MMC's in his study can be successfully correlated with high dislocation densities in those materials arising from the difference in the thermal expansion coefficients between the reinforcement and the matrix. The SiCw MMC's studied by Arsenault, however, possessed whiskers which were of much lower aspect ratio (l_i/d), on average ~ 4.2 when compared to those in the present study which were > 18, and, therefore, could not be considered to strengthen the MMC by shear transfer to the same degree.

Particle strengthening by Orowan looping has been used by Lederich and Sastry [4] to predict the strengths of their MMC's. However, in the present study the size (~ 0.7μm diameter) and therefore, the particle spacing of the particulate (~ 2.4μm) is too large to promote effective slip blockage and an increase in strength of less than 4MPa is predicted over the matrix value for the MMC using the simplest form of the Orowan equation to calculate the Orowan bowing stress:

$$\tau_{Orowan} = \mu b / \lambda \qquad (3)$$

where: μ = matrix shear modulus

b = Burgers vector

λ = the average particle spacing

For aluminum $b = 2.9 \times 10^{-10}$m and for the 6.35mm thick sheet μ = 27GPa, λ = 2.4μm. Nieh et al [9] have similarly concluded that the size and spacing of the SiC whiskers

and particulates in their Al alloy MMC's were too coarse to be effective barriers to dislocation motion. Materials containing non-deformable particles such as dispersion-hardened alloys have been termed 'plastically non-homogenous' by Ashby [24]. When such an alloy is deformed, gradients of deformation will occur in the matrix microstructure as this will plastically deform more than the particles. To accomodate these deformation gradients dense arrays of dislocations must be stored which are termed 'geometrically necessary' dislocations. The density of these dislocations for an alloy containing equi-axed particles, ρ^G is given by [24]:

$$\rho^G = \frac{2f}{d}\frac{4\gamma}{b} \tag{4a}$$

where:

$$\gamma = \tau_m / \mu \tag{4b}$$

γ = matrix shear strain

f = volume fraction of particles

d = average particle diameter

For the 6.35mm thick sheet particulate MMC, γ = 0.0057, f = 0.154, d = 0.65μm. This gives a value of ~3 x 10^{13} geometrically necessary dislocations. The strengthening from these dislocations, σ_G is given by [24]:

$$\sigma_G = \alpha\mu b\sqrt{\rho^G} \tag{5}$$

where: α = 0.34 for Al-Cu alloys [25]

Using the values above, equation (5) yields a value of ~15MPa. This increase alone does not account for the strength improvement of the SiCp MMC over the unreinforced matrix alloy. A value of 1.25 has been used for α obtained for pure aluminum [26] which would have the effect of increasing the strengthening contribution to ~55MPa alloy. This, however, is an overestimation of the strength as the value of α varies between alloys. If the dislocations stored from previous thermal treatments are also considered then the contribution from these assuming equi-axed particles is given by [26]:

$$\sigma_T = \alpha\mu\sqrt{\left(\frac{12f\epsilon b}{(1-f)}\left(\frac{1}{d}\right)\right)} \tag{6a}$$

where: $\varepsilon = \Delta CTE \times \Delta T$ (6b)

Using a value of $\Delta CTE = 1.94 \times 10^{-5} K^{-1}$ [26] and where f, b, α, μ, and d are defined above, the difference between the thermal expansion coefficients of the Al alloy and the SiC particles and $\Delta T = 470K$ (assuming quenching from solution heat treatment temperature) and the data above gives a value of ~28MPa.

If the strengthening contributions from Orowan looping, geometrically necessary dislocations and dislocations generated during quenching after heat treatment are added this predicts a strength increase over the matrix of ~47MPa. Although this correlates well with the experimental results for the 6.35 and 1.8mm as-fabricated sheets, the observed increase in the 3.18mm sheet was > 175MPa. As discussed earlier, the reason for this is unclear. Therefore, although there is some variability in the data these results suggest that the strengthening contributions due to the various particle/dislocation terms are additive and that the particulate MMC could be treated as a high volume fraction dispersion-hardened alloy. The work of Hansen and Ralph [27] on dispersion strengthened polycrystals would tend to support this argument. They have suggested that the strengthening contributions from dislocation densities associated with hardening due to particles and from work hardening of the matrix are additive and give a good approximation of stress-strain data.

The prediction of the Young's moduli of the MMC's is much simpler than predicting the strength as the modulus relies mostly on the volume fraction of the reinforcement and is less susceptible to microstructural effects, such as whisker clustering and voids. The Halpin-Tsai model [28] was modified to predict the Young's moduli. It was originally developed to predict the moduli of continuous fiber reinforced composites. Ashton, Halpin and Petit [29] have shown that the Halpin-Tsai model can be used for predicting the Young's moduli of a number of discontinuous fiber reinforced composites. The equations developed for predicting the transverse modulus of the composite account for different fiber cross-sectional shapes and packing geometry. The equations used in this study were formulated for fibers packed in a diamond array with rectangular cross-sections and were used to predict the longitudinal and transverse moduli of aligned discontinuous fibers. The following equations were used to calculate the moduli of interest [29]:

$$E_i = \sum_{\theta=0^\circ}^{\theta=90^\circ} f_o \left[E_m \left(1+\xi_i \eta_i V_f \right) / \left(1-\eta_i V_f \right) \right] \quad (6a)$$

where:

$$\eta_i = \left[\left(E_f / E_m \right) - 1 \right] / \left[\left(E_f / E_m \right) + \xi_i \right] \quad (6b)$$

and

$$\xi_i = 2 \left(l_i / d \right) \quad (6c)$$

i = longitudinal or transverse direction

f_o = % of whiskers of given orientation

E_i = composite Young's modulus

E_m = matrix Young's modulus

E_f = fiber Young's modulus

V_f = volume fraction of fibers

l_i = average fiber length

d = average fiber diameter or thickness

The moduli of the whisker MMC's were calculated using the projected whisker lengths and mean angles of the orientation increments between 0-90°. For the particulate MMC, the moduli were calculated independently using the appropriate l_i / d ratios. Due to the irregular, platelike morphology of the SiCp, the average value of the vertical and horizontal dimensions of each particle on the plane normal to the loading direction were used to represent the particle diameter, d, in the model. The length of the particulate, l_i, was taken as the projected distance onto a plane parallel to the loading direction. The moduli of the particulate and whisker SiC were assumed to be 410GPa [30] and 483GPa [22], respectively. Figures 13 to 15 show the predicted and experimental moduli for each material system in both the longitudinal and transverse directions. In each case the predicted moduli are within 7% of the measured moduli, with most comparisons being much closer. This would indicate that the microstructural details, e.g., whisker dimension and orientation, were accurately characterized.

The Halpin-Tsai model was used in this paper to predict the Young's modulus for all of the composite systems studied. There are several other rather simple models in the literature

that also give good correlation for either the particulate or the whisker reinforced composite but usually not both. These models are discussed in some detail in reference [31].

Conclusions

Room temperature tensile tests were conducted on an aluminum powder metallurgy alloy, both unreinforced and reinforced with SiC particulates or whiskers. The results of these tests were correlated with a microstructural study of the materials to predict the strengths and moduli of the MMC's. The predictions were within 7 and 16% of the observed behavior for the moduli and ultimate strengths, respectively. Improvements to the Young's moduli and ultimate strengths of the unreinforced matrix alloy were achieved by the addition of the SiC reinforcements. Fractographic evidence suggested that the interfacial bond between the matrix and the whiskers was good and that this, together with the high aspect ratio of the whiskers (> 18), promoted effective load transfer from the matrix to the whisker by shear transfer thus raising the ultimate strengths and moduli of the whisker reinforced MMC's. The particulate MMC contained particles with much lower aspect ratios (~1-2) than the whiskers and, therefore, were unable to transfer load from the matrix as effectively. Although there were inconsistences in the data the behavior of the particulate MMC more clearly approached that of a dispersion hardened alloy. Failure of the materials was predominantly by microvoid coalescence with the MMC's exhibiting shallow dimples and low ductilities due to constraint within the matrix exerted by the reinforcement which limited plastic flow.

Acknowledgements

This work was done while the first author held a National Research Council-NASA Research Associateship. The authors wish to thank Mr. Michael Holder of Advanced Composite Materials Corporation, Greer SC, who, while under a contract from NASA Langley Research Center, conducted the image analysis of the whisker MMC's.

References

1. R.J. Arsenault and R.M. Fisher, Scripta Met, 17 (1983), 67-71.

2. M. Vogelsang, R.J. Arsenault, and R.M. Fisher, Met Trans, 17A (1986), 379-389.

3. S.V. Nair, J.K. Tien, and R.C. Bates, Int Metals Revs, 30 (1985), 275-290.

4. R.J. Lederich and Sastry, Mats Sci Engng, 55 (1982), 143-146.

5. V.C. Nardone and K.M. Prewo, Scripta Met, 20 (1986), 43-48.

6. C.R. Harris and F.E. Wawner, Processing and Properties for Powder Metallurgy Composites, ed. P. Kumar, K. Vedula and A.Ritter (The Metallurgical Society, 1988), 107-116.

7. S.R. Nutt, Interfaces in Metal-Matrix Composites, ed. A.K. Dhingra and S. Fishman (The Metallurgical Society, 1986), 157-167.

8. D.L. McDanels and C.A. Hoffman, NASA TP-2302, July 1984.

9. T.G. Nieh, K. Xia and T.G. Langdon, J Engng Mats Tech, 110 (1988), 77-82.

10. T.G. Nieh and R.F. Karlak, J Mats Sci Lett, 2 (1983), 119-122.

11. C.R. Crowe, R.A. Gray and D.F. Hasson, 5th Int Conf Comp Mats, eds. W.C. Harrigan, Jr., J. Strife and A.K. Dhingra (The Metallurgical Society, AIME, 1985), 843-866.

12. T. Christman and S. Suresh, Acta Met, 36 (1988), 1691-1704.

13. J.M. Papazian, Met Trans, 19A (1988), 2945-2953.

14. T. Christman, A. Needleman and S. Suresh, Acta Met, 37 (1989), 3029-3050.

15. M. Manoharan and J.J. Lewandowski, Scripta Met, 23 (1989), 301-304.

16. S.H. Doong, T.C. Lee, I.M. Robertson and H.K. Birnbaum, Scripta Met, 23 (1989), 1413-1418.

17. R. Arone, O. Botstein and B. Shpigler, Israel J. Tech, 24 (1988), 393-399.

18. S.R. Nutt, J Amer Ceram Soc, 67 (1984), 428-431.

19. R.J. Arsenault and C.S. Pande, Scripta Met, 18 (1984), 1131-1134.

20. J.R. Vinson and T.W. Chou,"Composite Materials and Their Use in Structures," Applied Sci Pubs (1975), 356-362.

21. A. Kelly and W.R. Tyson, J Mechs Phys Sols, 13 (1965), 329-350.

22. M.D. Skibo, Report SAND81-8212, Sandia National Laboratories, 1981.

23. R.J. Arsenault, Mats Sci Engng, 64 (1984), 171-181.

24. M.F. Ashby, Phil Mag, 21 (1970), 399-424.

25. J.W. Martin, "Micromechanisms in particle-hardened alloys," Cambridge Univ Press (1980), 88.

26. R.J. Arsenault and N. Shi, Mats Sci Engng, 81 (1986), 175-187.

27. N. Hansen and B. Ralph, Acta Met, 34 (1986), 1955-1962.

28. J.C. Halpin and S.W. Tsai, (Report AFML TR 67-423).

29. J.E. Ashton, J.C. Halpin and P.H. Petit, "Primer on Composite Materials: Analysis," Progress in Mats Sci Series, III (Technomic, 1969), 77-85

30. H.E. Rosinger, I.G. Ritchie and A.J. Shillinglaw, Mats Sci Engng, 16 (1974), 143-154.

31. W.S. Johnson and M.J. Birt, To be submitted to J Comps Tech Res, (1990).

TABLE I - AVERAGE SIZES OF SiC PARTICLES FOR THE PARTICULATE MMC SHEETS.

Sheet Thickness (mm)	Length, L (μm)	Width, T (μm)	Thickness, S (μm)
6.35	1.03	0.71	0.60
3.15	0.78	0.58	0.56
1.8	0.67	0.60	0.49

Data represent the average values of measurements of >1000 SiC particles/sheet.

TABLE II - TENSILE PROPERTIES FOR THE MATERIALS

Material and Plate thickness		Proportional Limit (MPa)		Ultimate Strength (MPa)		Elongation (%)		Youngs' Modulus (GPa)	
Test		1	2	1	2	1	2	1	2
Matrix									
6.35mm	L-T	166	167	303	312	10.9	13.7	72	72
	T-L	171	162	293	312	12.3	12.0	71	73
3.18mm	L-T	186	-	281	-	10.0	-	74	-
	T-L	200	-	274	-	7.4	-	74	-
1.8mm	L-T	228	-	363	-	10.8	-	73	-
	T-L	261	-	360	-	8	-	72	-
15v/o SiCp									
6.35mm	L-T	219	218	350	355	3.0	4.6	100	101
	T-L	210	222	343	338	5.3	4.8	99	116
3.18mm	L-T	334	312	453	459	5.0	5.8	103	99
	T-L	303	302	426	457	4.6	5.8	99	102
1.8mm	L-T	281	290	409	427	3.5	4.2	91	92
	T-L	270	276	396	420	2.8	4.5	95	95
15v/o SiCw									
6.35mm	L-T	202	-	432	-	2.6	-	112	-
	T-L	182	184	367	360	5.9	5.7	92	102
3.18mm	L-T	221	218	446	424	3.0	2.9	115	106
	T-L	196	197	325	331	4.1	5.7	97	94
1.8mm	L-T	230	237	574	561	3.5	3.1	110	105
	T-L	228	214	443	444	6.0	6.2	98	92
30v/o SiCw									
6.35mm	L-T	192	-	491	-	0.9	-	137	-
	T-L	187	-	496	-	2.2	-	117	-
3.18mm	L-T	233	234	434	545	0.7	1.3	142	131
	T-L	226	234	496	492	1.7	1.8	122	123
1.8mm	L-T	246	217	543	563	2.9	3.8	118	121
	T-L	243	231	535	563	2.0	2.7	129	127

Results are from single or duplicate tests as indicated.

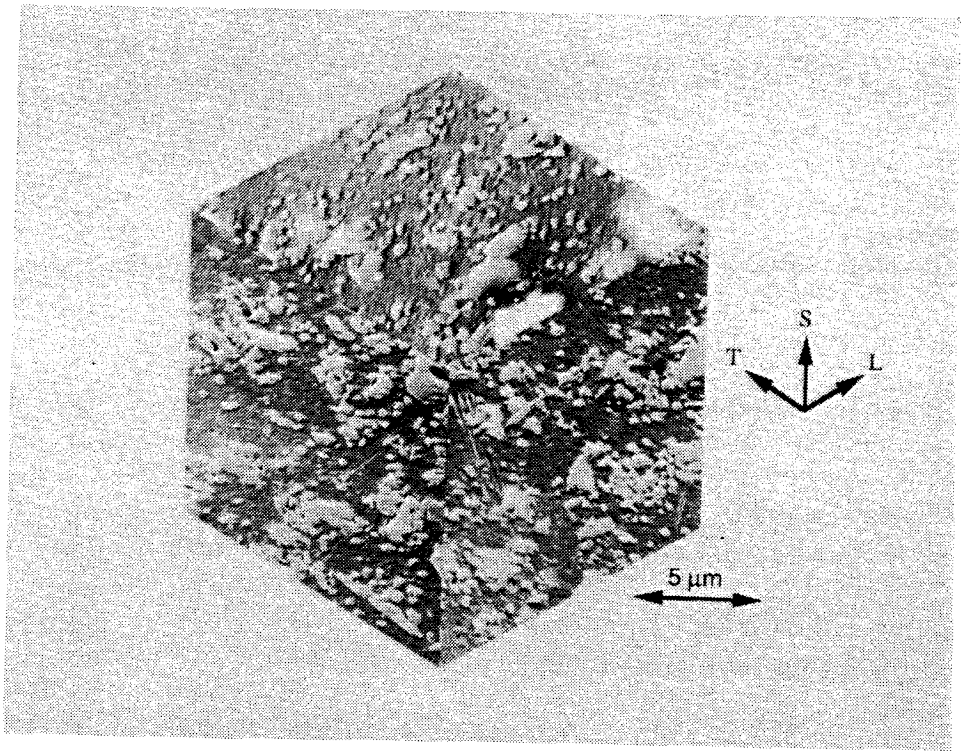

Figure 1 - Typical Microstructure of the 15 v/o Particulate MMC (1.8mm sheet thickness).

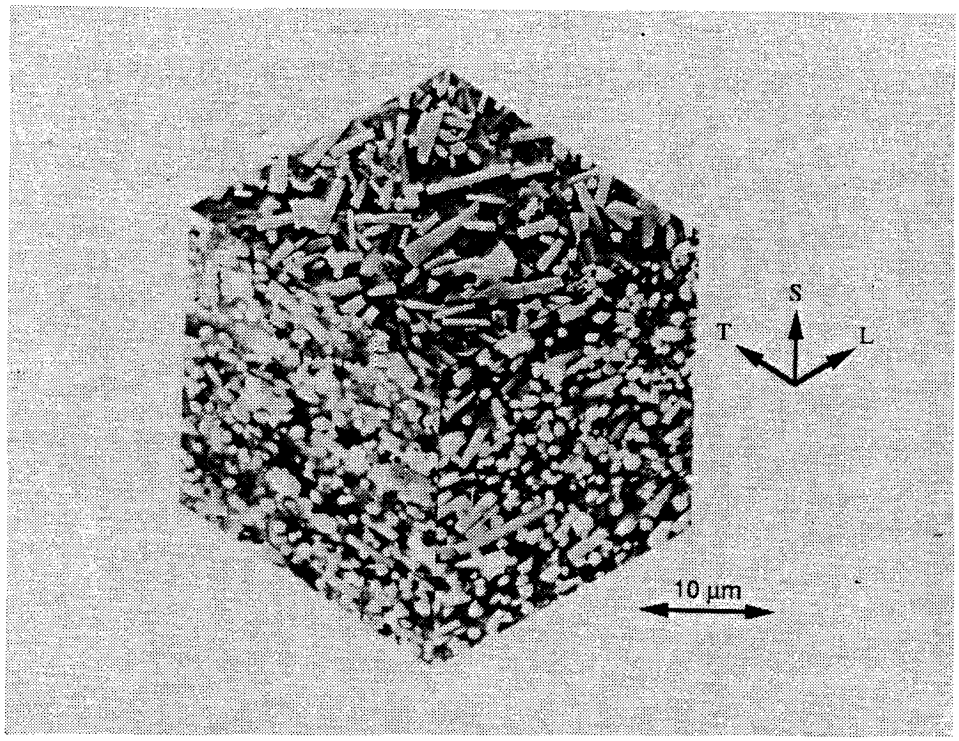

Figure 2 - Typical Microstructure of the 15 v/o Whisker MMC (1.8mm sheet thickness).

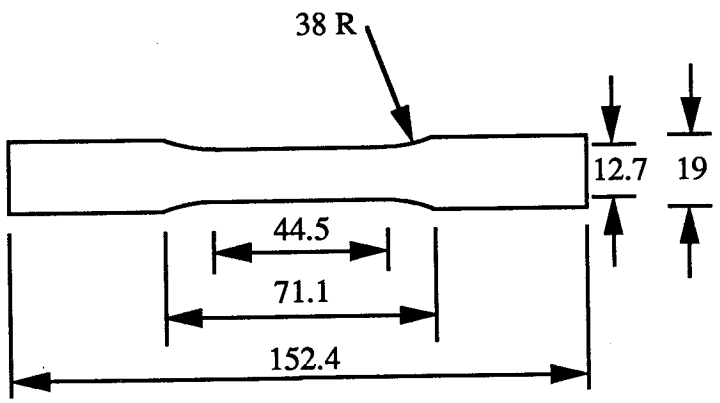

Figure 3 - Tensile Test Specimen (All dimensions are in mm)

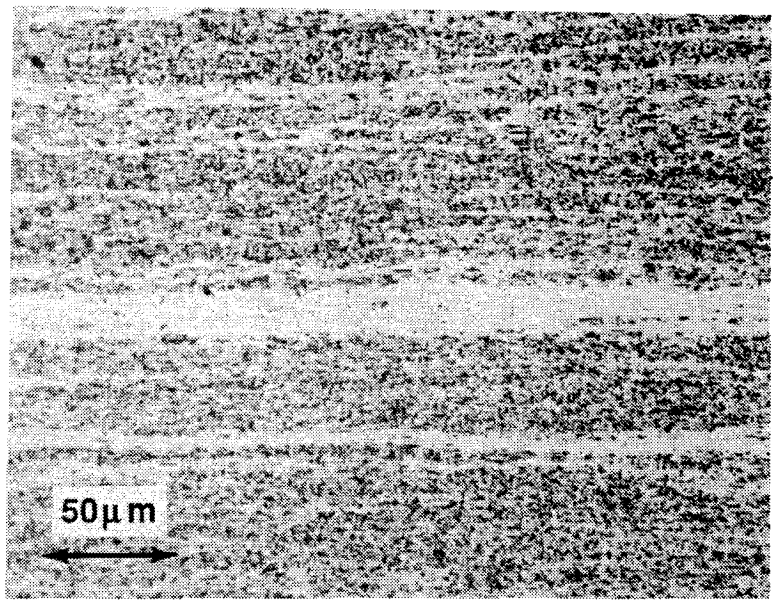

Figure 4 - Optical Micrograph of Macroscopic Banding in the 6.35mm thick sheet of the 15 v/o SiC Whisker MMC (Transverse plane, extrusion direction right to left).

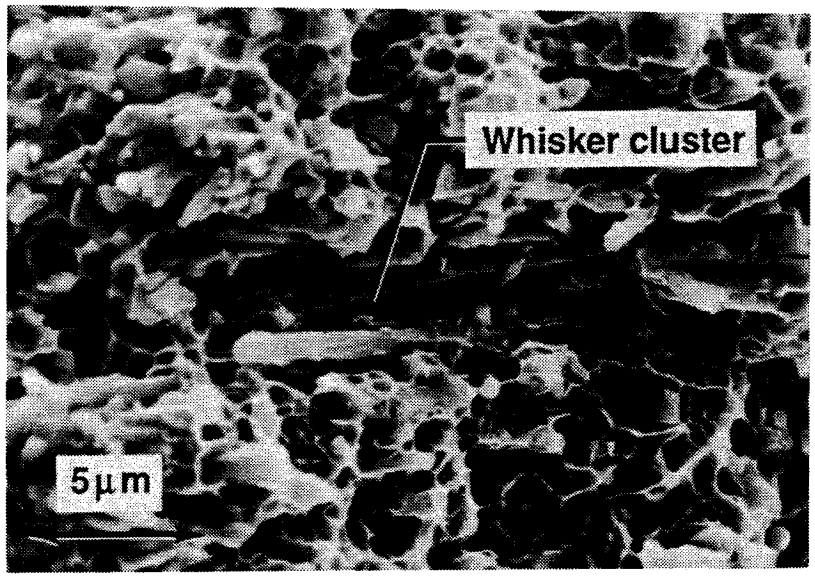

Figure 5 - SEM Fractograph of a Whisker Cluster in the 30 v/o Whisker MMC.

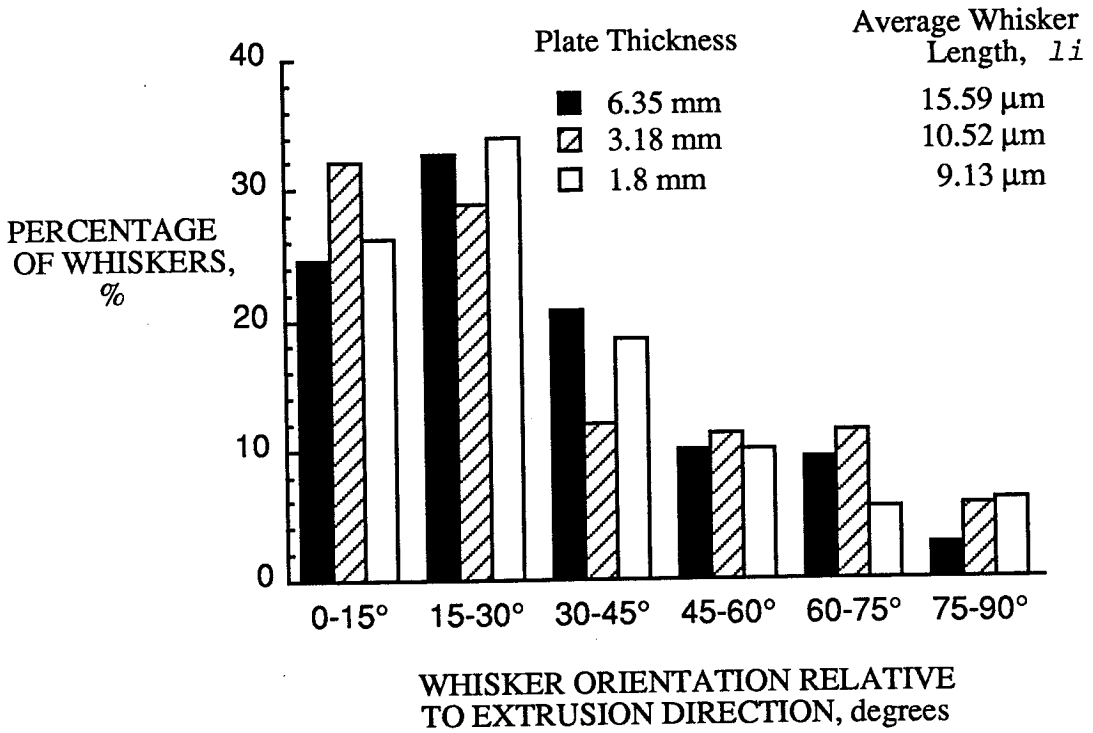

Figure 6 - Distributions of Whisker Orientations and Average Whisker Lengths for the 15 v/o Whisker MMC.

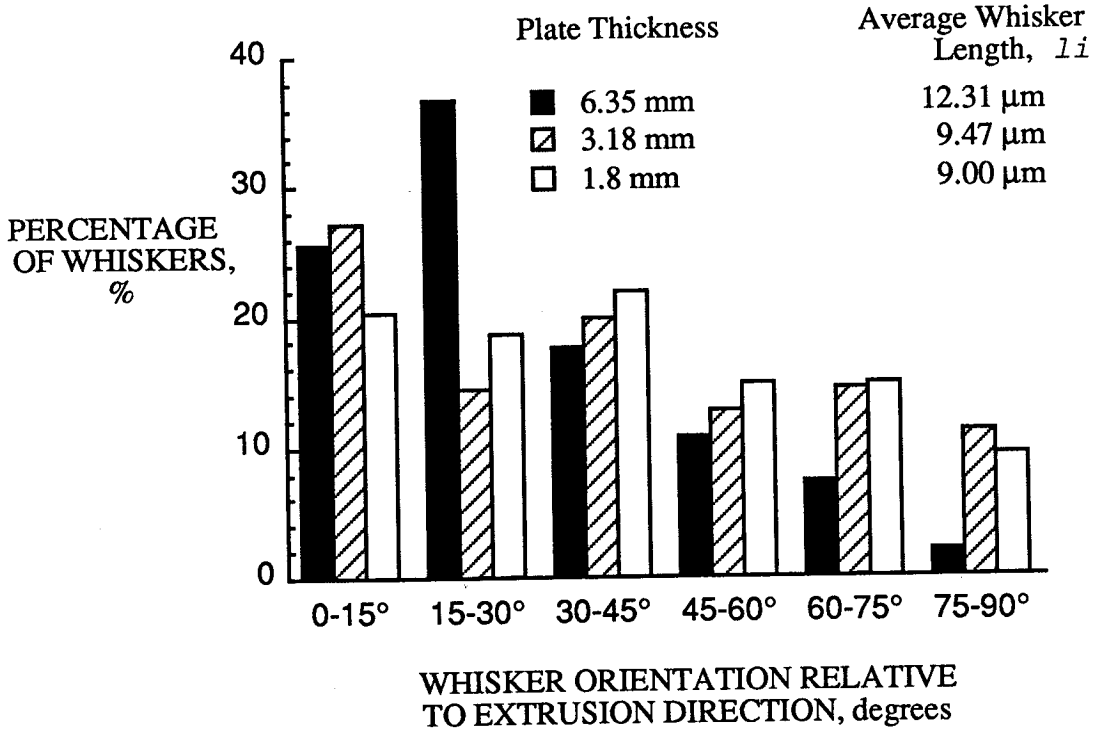

Figure 7 - Distributions of Whisker Orientations and Average Whisker Lengths for the 30 v/o Whisker MMC.

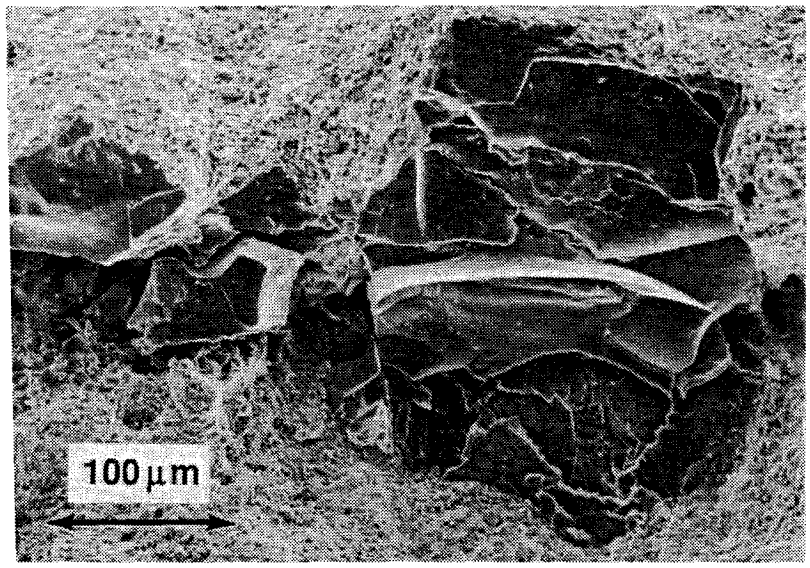

Figure 8 - SEM Fractograph of an Al-Cu Powder Particle on the Surface of the 15 v/o Whisker MMC.

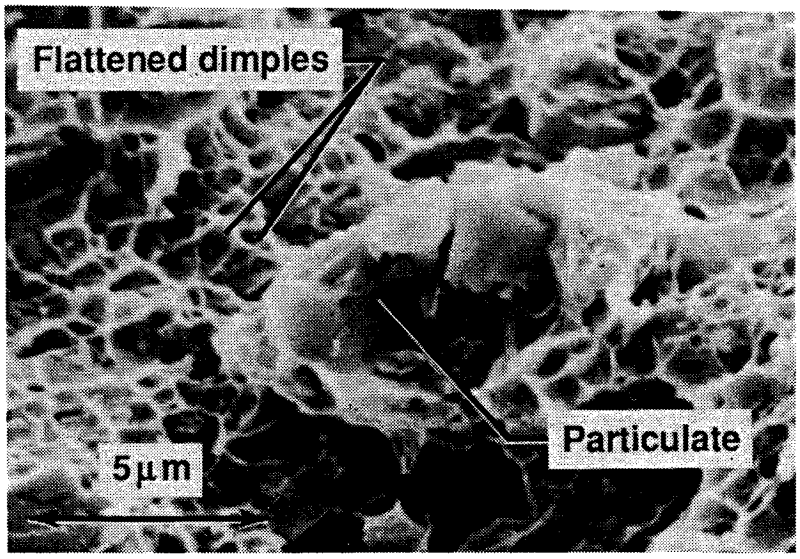

Figure 9 - SEM Fractograph of SiC Particles on the Surface of the 15 v/o Particulate MMC.

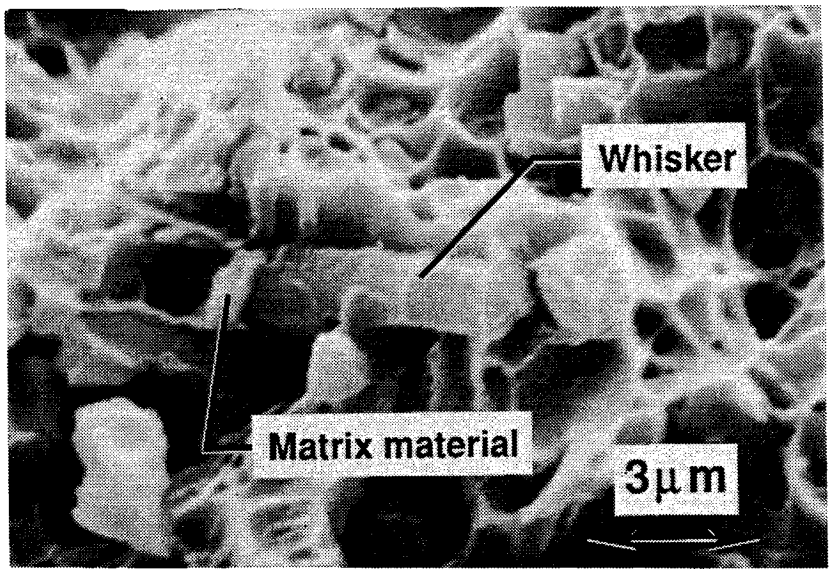

Figure 10 - SEM Fractograph of a Whisker at the Base of a Dimple in the 15 v/o Whisker MMC.

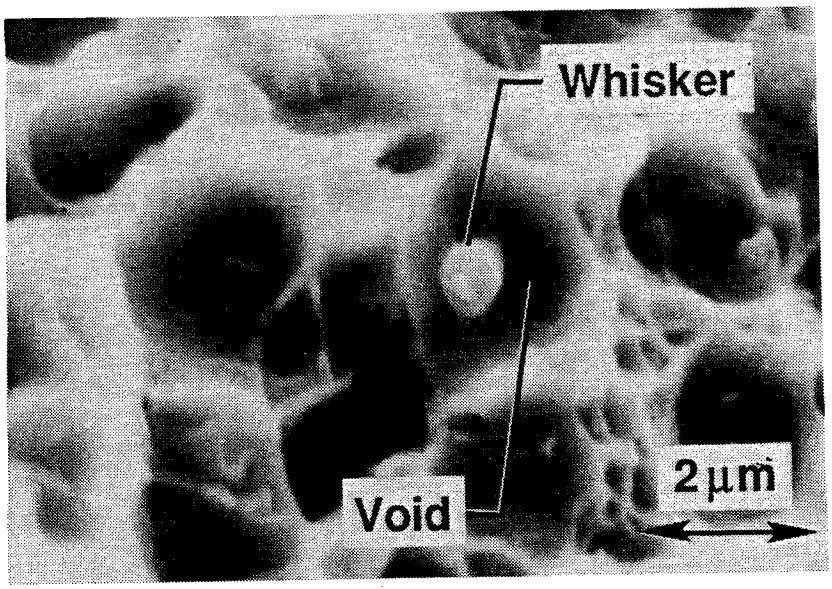

Figure 11 - SEM Fractograph of Al Matrix Material attached to a Whisker in the 15 v/o Whisker MMC.

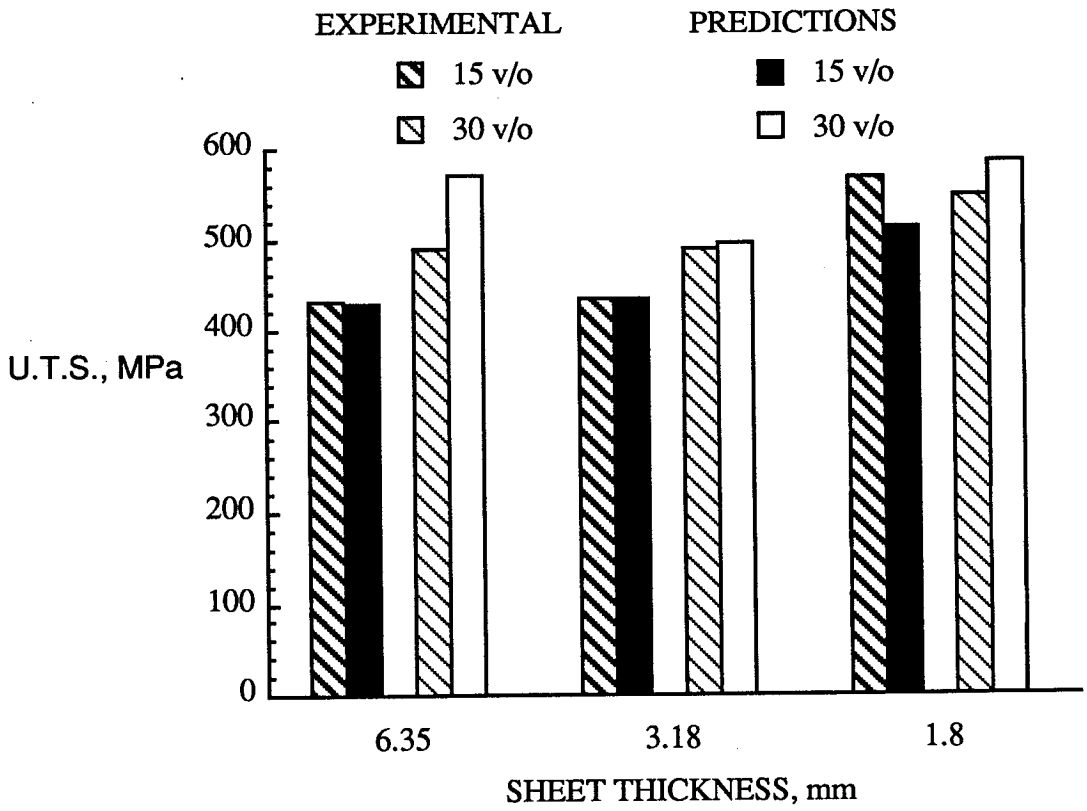

Figure 12 - Predictions of Ultimate Tensile Strengths with Experimental Data for the Whisker MMC's in the L-T Orientation.

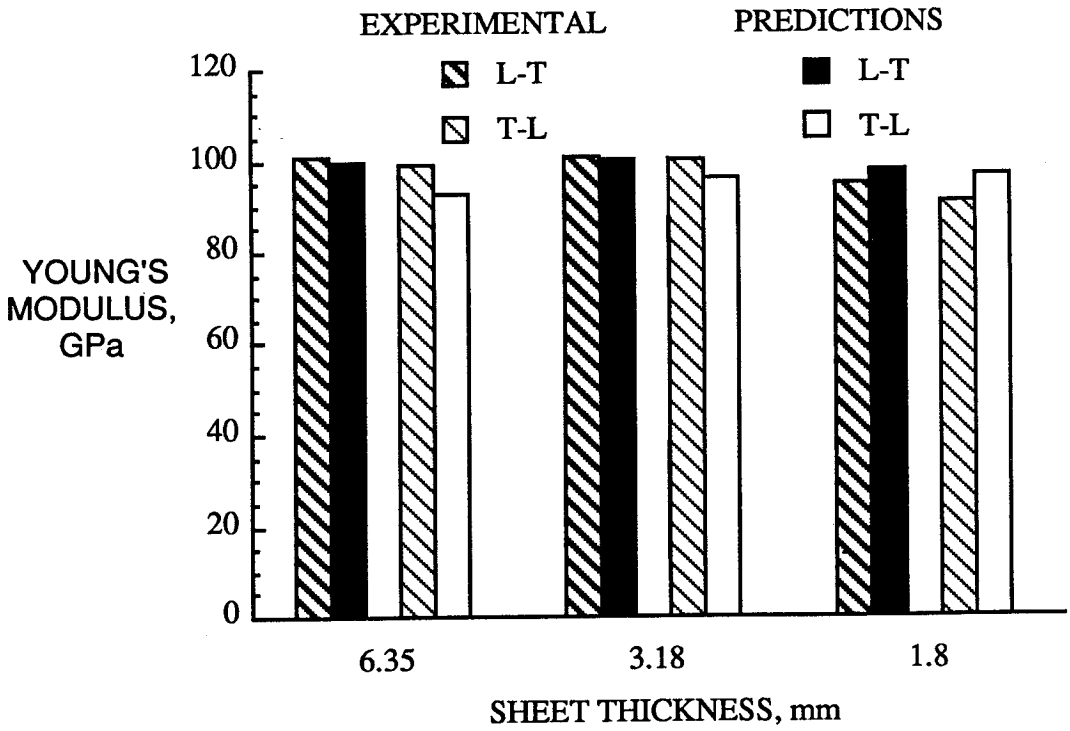

Figure 13 - Predictions of Young's Moduli with Experimental Data for the Particulate MMC's in the L-T and T-L Orientations.

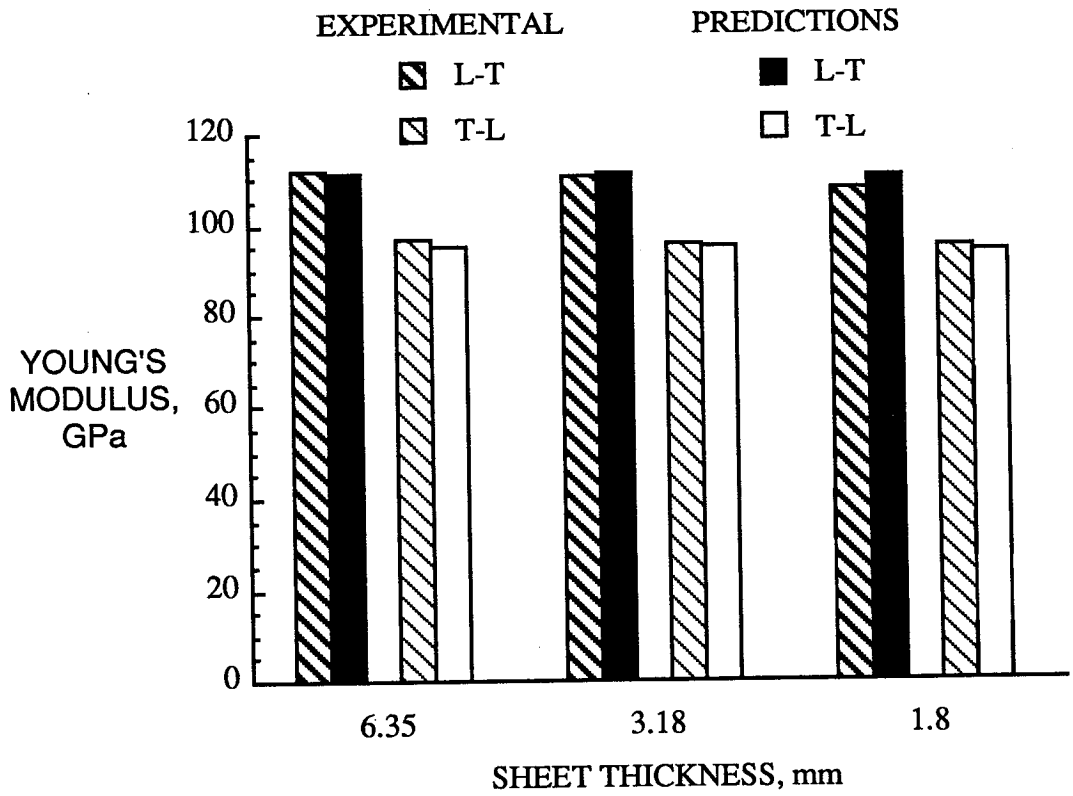

Figure 14 - Predictions of Young's Moduli with Experimental Data for the 15 v/o Whisker MMC's in the L-T and T-L Orientations.

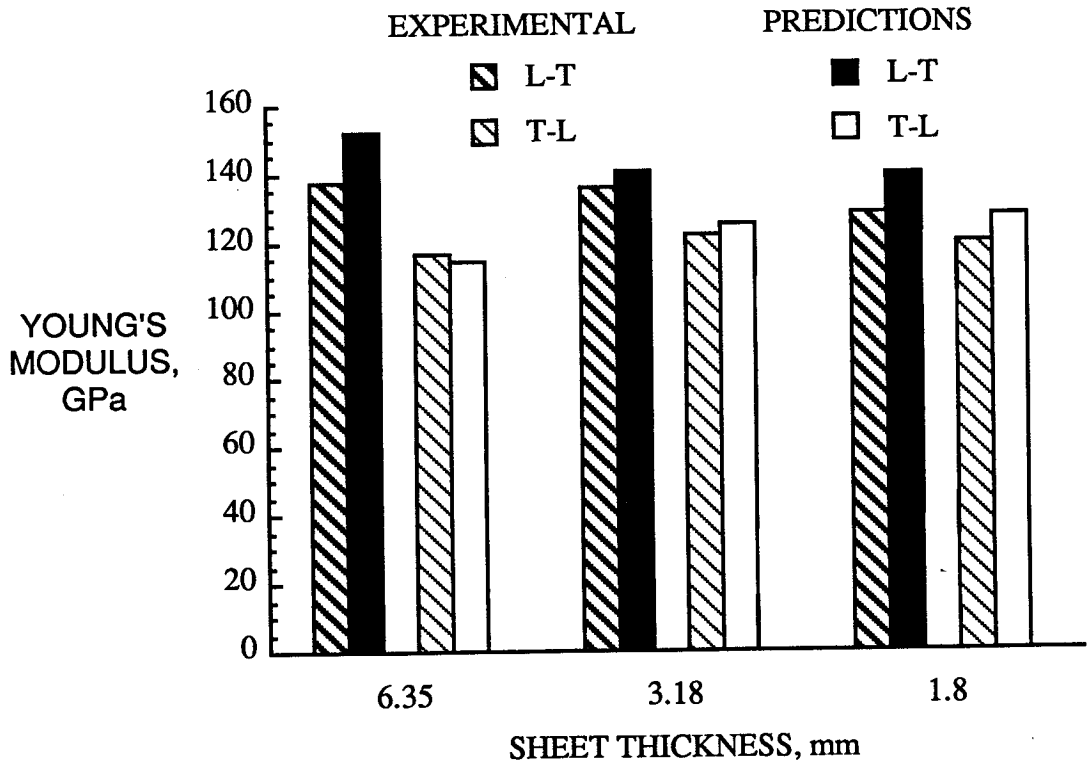

Figure 15 - Predictions of Young's Moduli with Experimental Data for the 30 v/o Whisker MMC's in the L-T and T-L Orientations.

NASA
National Aeronautics and Space Administration

Report Documentation Page

1. Report No.	2. Government Accession No.	3. Recipient's Catalog No.
NASA TM-102694		

4. Title and Subtitle	5. Report Date
The Influence of Microstructure on the Tensile Behavior of an Aluminum Metal Matrix Composite	July 1990
	6. Performing Organization Code

7. Author(s)	8. Performing Organization Report No.
Michael J. Birt and W. Steven Johnson	
	10. Work Unit No. 506-43-71-03

9. Performing Organization Name and Address	11. Contract or Grant No.
NASA Langley Research Center, Hampton, VA 23665-5225	
	13. Type of Report and Period Covered: Technical Memorandum

12. Sponsoring Agency Name and Address	14. Sponsoring Agency Code
National Aeronautics and Space Administration Washington, DC 20546-0001	

15. Supplementary Notes

Michael J. Birt, Analytical Services and Materials, Inc., Hampton, VA
W. S. Johnson, NASA Langley Research Center, Hampton, VA 23665-5225

16. Abstract

The relationship between tensile properties and microstructure of a powder metallurgy aluminum alloy, 2009 has been examined. The alloy was investigated both unreinforced and reinforced with 15 v/o SiC whiskers or 15 v/o SiC particulate to form a discontinuous metal matrix composite (MMC). The materials were investigated in the as-fabricated condition and in three different hot-rolled sheet thicknesses of 6.35, 3.18, and 1.8mm. Image analysis was used to characterize the morphology of the reinforcements and their distributions within the matrix alloy. Fractographic examinations revealed that failure was associated with the presence of microstructural inhomogeneities which were related to both the matrix alloy and to the reinforcement. The results from these observations together with the matrix tensile data were used to predict the strengths and moduli of the MMC's using relatively simple models. The whisker MMC could be modeled as a short fiber composite and an attempt was made to model the particulate MMC as a dispersion/dislocation hardened alloy.

17. Key Words (Suggested by Author(s))	18. Distribution Statement
Metal matrix composite Silicon carbide Aluminum alloy Mechanical properties Modeling	Unclassified - Unlimited Subject Category - 24

19. Security Classif. (of this report)	20. Security Classif. (of this page)	21. No. of pages	22. Price
Unclassified	Unclassified	28	A03